

PRELIMINARY STUDY TO GENERATE A DEM OF AMUNDSEN BAY, ANTARCTICA BY INTERFEROMETRIC SAR

Koichiro DOI¹, Taku OZAWA¹, Kazuo SHIBUYA¹, Hiroyuki NAKAGAWA²,
Makoto OMURA³ and Katsuaki KOIKE⁴

¹*National Institute of Polar Research, Kaga 1-chome, Itabashi-ku, Tokyo 173-8515*

²*Geographical Survey Institute, Kitasato 1, Tsukuba 305-0811*

³*Kochi Women's University, 5-15, Eikokuji-cho, Kochi 780-8515*

⁴*Kumamoto University, Kurokami 2-chome, Kumamoto 860-8555*

Abstract: A SAR interferogram was obtained from two JERS-1 SAR data sets around Amundsen Bay, west Enderby Land, received at Syowa Station on November 26, 1996 and January 9, 1997. Fringes were found in the interferogram related to topographic height and surface displacements. However, we could not generate a digital elevation model for the area because we did not succeed in carrying out phase unwrapping to estimate absolute phase. We compared the fringe patterns obtained for Tonaugh Island with the topographic map derived from the aerial photographs. Relative heights in the area of flat topography were estimated from the interferogram; the interferogram's fringes agreed with the contour line shapes on the topographic map.

key words: SAR, interferometry, DEM, JERS-1, Amundsen Bay

1. Introduction

Synthetic Aperture Radar (SAR) is a radar remote sensing sensor. High resolution of the image is obtained by pulse compression and the synthetic aperture technique. SAR data consist of amplitude and phase of backscattered microwaves. As the amplitude is affected by some characteristics of the ground surface due to the back-scattering mechanism, the SAR amplitude (intensity) image has been used to estimate vegetation, moisture distribution, surface characteristics of the ice sheet and sea ice signatures.

SAR interferometry makes use of the phase signal of the SAR data. To generate a SAR interferogram, more than two scenes which contain the same area are required. In the case of spaceborne SAR interferometry, the phase signals are derived from data obtained in repeat passes. The phase difference is caused by the difference in the microwaves propagation ranges. Three dimensional information on the earth's surface such as topographic height and surface deformations may be extracted from the phase differences. Therefore, by differentiating the interferograms, we can generate a digital elevation model (DEM) of remote regions such as the Arctic and Antarctic ice sheets.

Besides DEM generation, SAR interferometry is applied to detect ground surface deformation caused by large earthquakes (e.g. MASSONET *et al.*, 1993) and ice sheet

motion (*e.g.* KWOK and FAHNESTOCK, 1996).

To use SAR interferometry, observation geometry must be known precisely. Thanks to progress in tracking and navigation techniques for spacecraft and determination of satellite orbits, the SAR observation geometry is determined with high precision. This in turn makes it possible to do spaceborne SAR interferometry easily.

At the present time, the SAR sensors are operated by the satellites JERS-1, ERS-1, ERS-2, and RADARSAT. The multipurpose satellite receiving antenna at Syowa Station has been acquiring SAR data from JERS-1, ERS-1 and ERS-2 since 1991. The recurrence period of JERS-1 is 44 days and that of ERS-1/-2 is 35 days. Transmitted radar wavelengths of JERS-1 and ERS-1/-2 are 23.5 cm (L-band) and 5.6 cm (C-band), respectively. A mission data recorder is on board JERS-1, so SAR data observed in the Antarctic region can be recorded on the recorder and transmitted later to receiving stations far from Antarctica. Unfortunately, the recorder was dead at the end of 1997.

We have been generating a DEM around Syowa Station and study area of the Japanese Antarctic Research Expedition (JARE) using JERS-1, ERS-1, and ERS-2 SAR data. The JERS-1 SAR interferogram of the area around Amundsen Bay has been obtained for the first time. In the interferogram, topography and topographic changes due to deformation are contained in the fringes simultaneously. In this paper, we show details of the derived interferogram and result of comparison with an existing topographic map.

2. Outline of Interferometric SAR Processing

The principle of interferometric SAR has been mentioned in several papers (*e.g.* ZEBKER and GOLDSTEIN, 1986; LI and GOLDSTEIN, 1990), and details of the processing are also described in GENS and VAN GENDEREN (1996). We will mention only an outline of the processing, here.

The outline of the interferometric SAR processing is as follows (see also Fig. 1): First, we prepare two sets of CEOS formatted SAR raw data which include the same area. The data are processed by a SAR processor to make a SAR complex image called a single look complex (SLC). Next, a co-registration process is performed by affine transformation in order to match the pixels of the slave SLC to the corresponding pixels of the master SLC. Finally, phase differences between the two SLCs for each pixel are obtained by the following formula:

$$\Delta\Phi = \tan^{-1} \left[\frac{\text{Im}(S_1 \cdot S_2^*)}{\text{Re}(S_1 \cdot S_2^*)} \right], \quad (1)$$

where S_1 and S_2 are complex signals of a master SLC pixel and a slave pixel, respectively. Im means the imaginary part of the complex signal and Re means the real part. An asterisk means taking the complex conjugate.

In the above processing, Doppler frequency estimation and auto-focusing process are also executed in the process of generating an SLC.

An image of the phase differences between the two SLCs, which is called an interferogram, contains phase differences due to the slant range difference between the

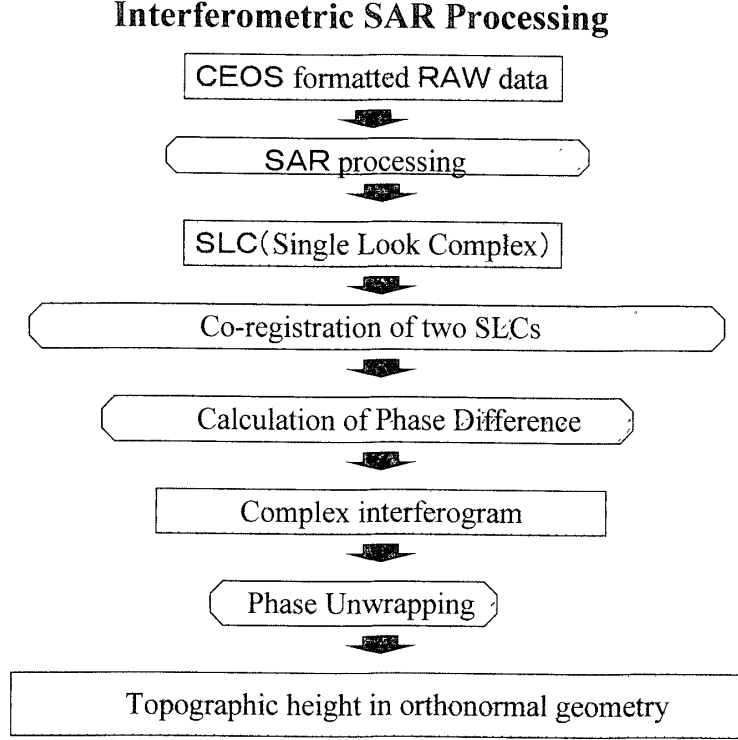


Fig. 1. Schematic flow of interferometric SAR processing.

two SLCs and due to topographic height and its changes. The phase difference induced by the slant range difference, which is called an orbital fringe, can be removed using orbital information. After removal of the orbital fringe, the remaining phase differences are induced by the surface topographic height and by the surface displacement. The phase difference $\Delta\Phi_T$ caused by topographic height (h) is as follows (e.g. URAI and YAMAGUCHI, 1996):

$$\Delta\Phi_T = \frac{4\pi h B \cos(\theta - \alpha)}{\lambda \rho \sin \theta} + 2\pi N + C, \quad (2)$$

where B is the baseline length between two antenna, θ is the off-nadir angle, α is the baseline tilt angle, λ is radar wave length, ρ is slant range, and N is an integer. On the other hand, the phase difference $\Delta\Phi_D$ induced by surface displacement is

$$\Delta\Phi_D = \frac{4\pi \Delta h}{\lambda \cos \theta} + 2\pi N + C, \quad (3)$$

where Δh is upward surface displacement.

Although, the observed phase difference takes values from zero to 2π radians, the true phase difference can take phase values greater than 2π . In an interferogram, integer multiples of 2π , that is N in eqs. (2) and (3), are wrapped and solving the integer multiples is called phase unwrapping. Phase unwrapping is necessary to estimate absolute topographic height and surface displacements, but it is difficult to do successful-

ly without several ground control points (GCPs) in many cases.

3. Interferogram

For the interferometric SAR processing, we employed SAR data observed by JERS-1 on November 26, 1996 and January 9, 1997 around Amundsen Bay, west Enderby Land. Using the two SAR data sets, two SLCs were made. The observed area is shown in Fig. 2. The employed data were received by the Alaska SAR Facility, Fairbanks and were transported to NASDA/EOC, Hatoyama. The CEOS formatted raw data were provided by NASDA/EOC.

SAR amplitude (intensity) images observed on November 26, 1996 and January 9, 1997 are shown in Figs. 3a and 3b, respectively. Details of the orbital information provided by RESTEC are indicated in Table 1. An interferogram generated from the two SLCs is shown in Fig. 4 superimposed on the amplitude image. Interferometric SAR software developed by Gamma Corporation was applied to obtain the interferogram.

In this interferogram, fringes due to topographic height and surface displacements are superimposed. Fringes on bare rock regions like the Mt. Riiser-Larsen and Tonaugh Island, which are indicated by indexes A and B, respectively, are considered to be induced by topographic height. On the other hand, those appearing in the east and west regions of the Mt. Riiser-Larsen, indicated by indexes C and D, respectively, may

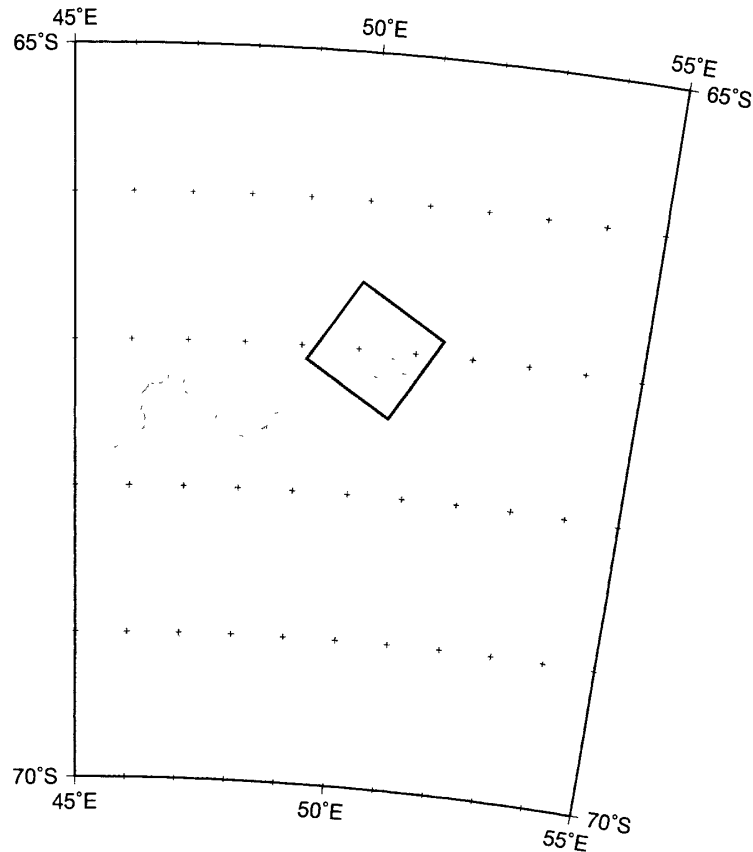


Fig. 2. Location of observed area.



Fig. 3a. JERS-1 SAR amplitude (intensity) image acquired on November 26, 1996.



Fig. 3b. JERS-1 SAR amplitude image acquired on January 7, 1997.

Table 1. Orbital information.

JERS-1 SAR PATH 171 ROW 414

	Master	Slave
Observation time (UT)	1996-11-26 0524:07	1997-01-09 0523:52
Flight alt. (m)	598608.769	598336.684
Slave alt. shift (m)		272.085
Baseline distance (m)		460.204
Height/contour (m)		109.869
Day distance (day)		44

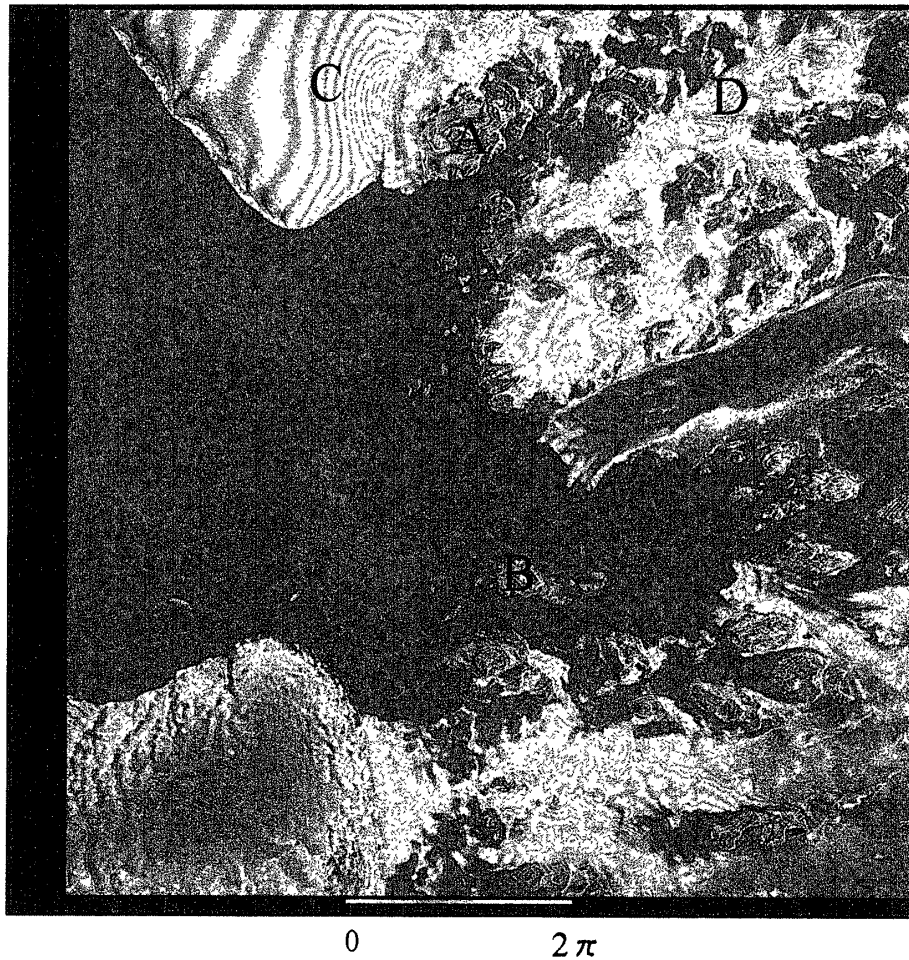


Fig. 4. Interferogram formed from the JERS-1 SAR data.

be induced by the ice sheet motion due to three-dimensional displacement. Under flat topography within the resolution of topographic limitation obtained by JERS-1 interferogram, for instance, approximately 100 m, fringes in region C correspond to shortening the slant range, which means uplift movements of the region toward the antenna. This region is the outer side of a turning point of a glacier and some stress may exist in the westward direction. Because a fringe pattern is affected by local changes of

backscattering coefficients, the obtained result must be ground-truthed to ascertain its nature. Fringes in region D are considered to be due to slow flow of the ice sheet. We guess the flow rate to be less than 50 m per year. These displacements will be discussed further in future articles.

4. Comparison of Height Inferred from Derived Fringe with Topographic Map

Unfortunately, we could not generate a digital elevation model, even for limited bare rock areas, from the interferogram, because of the lack of GCPs. In this section, to estimate accuracy of the derived interferogram, we compare heights inferred from the derived fringes on Tonaugh Island with a topographic map depicted from aerial photographs (MORIWAKI, 1996, private communication).

Figure 5 shows an enlarged interferogram for Tonaugh Island, corresponding to the topographic map of the island in Fig. 6. From Table 1, one cycle of the fringe is identical to 110 m. Relative heights above sea level estimated from the fringe image and topographic heights of corresponding points are indicated in Table 2. The points (A–J) are indicated both in Figs. 5 and 6. The mean difference is 17 m and the r.m.s. is 23 m. In this table, we can see that height differences at two peaks (C and D) are large; those at other points, which are located on relatively flat topography, are less than 20 m.

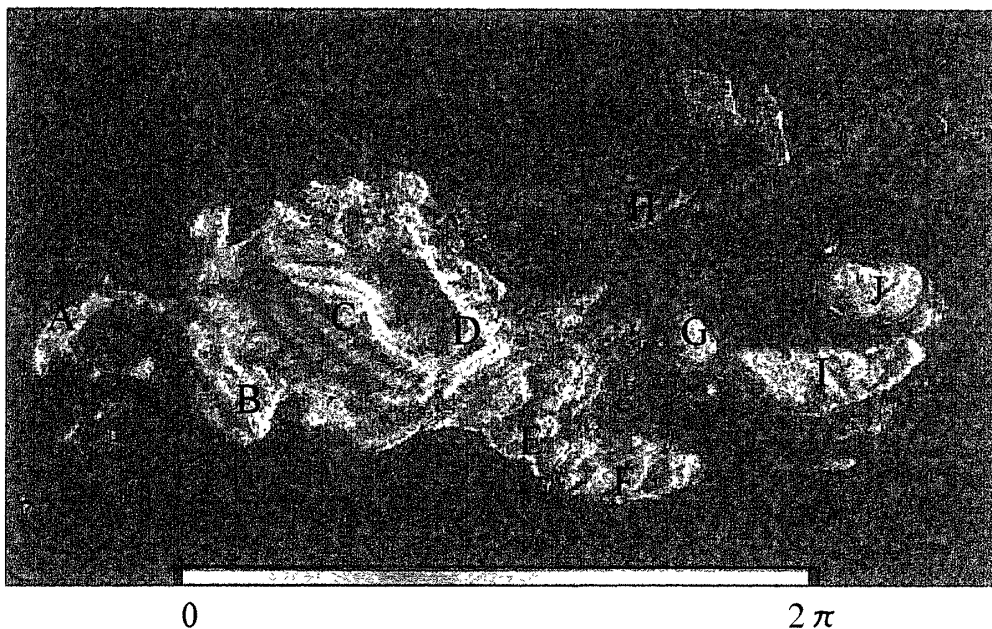


Fig. 5. Enlarged interferogram for Tonaugh Island.

5. Summary

We tried to generate a digital elevation model around Amundsen Bay by means of SAR interferometry using SAR data sets observed by JERS-1 on November 26, 1996 and

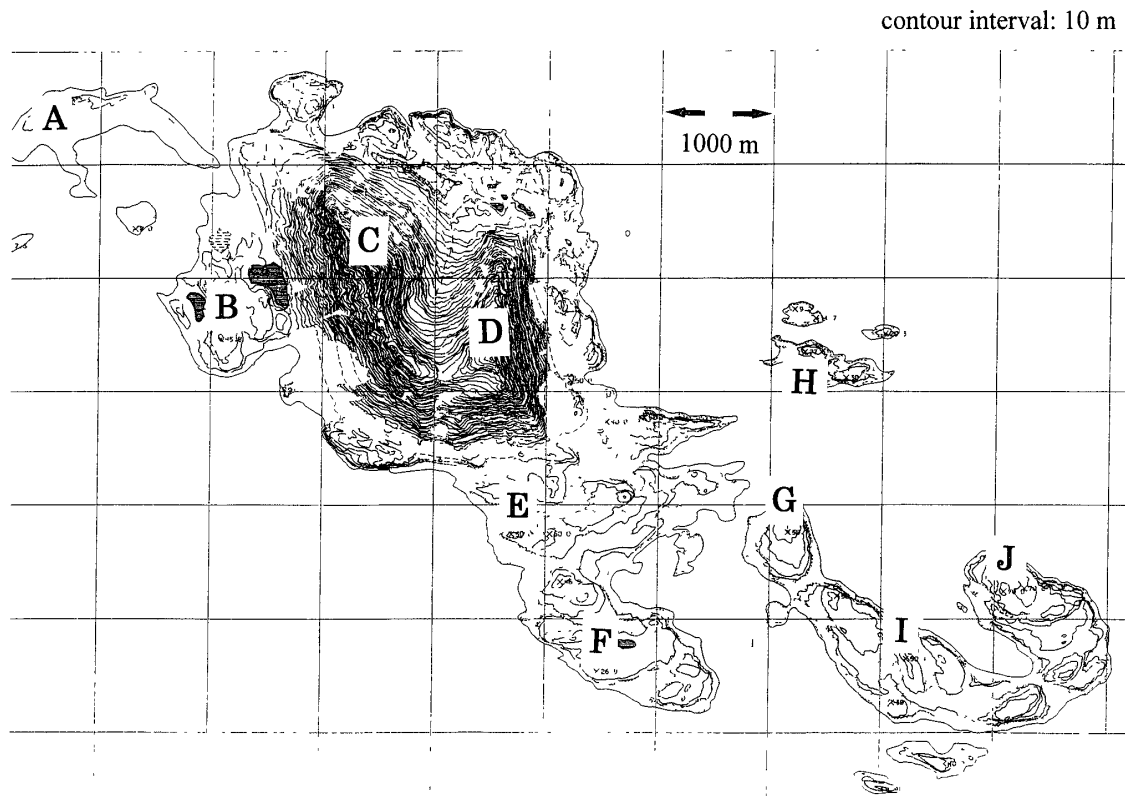


Fig. 6. Topographic map of Tonaugh Island (MORIWAKI, 1996, private communication).

Table 2. Comparison of heights from interferogram with those from topographic map.

Index in map	Height from map (m)	Height from interferogram (m)	Difference (m)
A	27	20	7
B	46	60	14
C	510	430	80
D	460	430	30
E	50	60	10
F	27	30	3
G	50	50	0
H	27	10	17
I	50	60	10
J	70	70	0

January 9, 1997. An interferogram was obtained and fringes induced by topographic height and surface displacements appear in it. To generate a digital elevation model, absolute phases must be estimated by carrying out phase unwrapping. Unfortunately, we could not perform the phase unwrapping in this study because there are no GCPs. We compared topographic heights derived from the interferogram for Tonaugh Island with those from the topographic map. The heights estimated from the interferogram

indicate good agreement with those from the topographic maps at points on the flat topography area.

In the next study, we will try to generate a digital elevation model around Amundsen Bay by finding several appropriate GCPs. We also plan to carry out ground truth experiments using radar reflectors with GPS receivers to form appropriate GCPs.

Acknowledgments

MITI and NASDA own the JERS-1 data. The authors thank NASDA/EOC and RESTEC for providing JERS-1 data and JERS-1 orbit information. Sincere thanks are extended to Drs. M. TOBITA and S. FUJIWARA of the Geographical Survey Institute for their valuable advice on generating the SAR interferogram.

References

- GENS, R. and VAN GENDEREN, J.L. (1996): SAR interferometry-issues, techniques, applications. *Int. J. Remote Sensing*, **17**, 1803–1835.
- KWOK, R. and FAHNESTOCK, M. (1996): Ice sheet motion and topography from radar interferometry. *IEEE Trans. Geosci. Remote Sensing*, **34**, 189–200.
- LI, F. and GOLDSTEIN, R.M. (1990): Studies of multibaseline spaceborne interferometric synthetic aperture radars. *IEEE Trans. Geosci. Remote Sensing*, **28**, 88–97.
- MASSONET, D., ROSSI, M., CARMONA, C., ADRAGNA, F., PELTZER, G., FEIGL, K. and RABAUTE, T. (1993): The displacement field of the Landers earthquake mapped by radar interferometry. *Nature*, **364**, 138–142.
- URAI, M. and YAMAGUCHI, Y. (1996): Applications of differential synthetic aperture radar interferometry to the earth sciences: Potential for geothermal reservoir monitoring. *Chishitsu Chosajo Geppo (Bull. Geol. Surv. Jpn.)*, **47**, 23–31 (in Japanese with English abstract).
- ZEBKER, H. and GOLDSTEIN, R.M. (1986): Topographic mapping from interferometric synthetic aperture radar observation. *J. Geophys. Res.*, **91**, 4993–4999.

(Received March 3, 1998; Revised manuscript accepted June 12, 1998)